Direct experimental observation of the Frenkel line in supercritical neon

C. Prescher[1], Yu. D. Fomin[2], V. B. Prakapenka[3], J. Stefanski[1], K. Trachenko[4] and V.V. Brazhkin[2]
[1] *Institut für Geologie und Mineralogie, Universität zu Köln, 50939 Köln, Germany*
[2] *Institute for High Pressure Physics, Russian Academy of Sciences, Troitsk 142190, Moscow, Russia*
[3] *Center for Advanced Radiation Sources, University of Chicago, Chicago, Illinois 60637, USA and*
[4] *School of Physics and Astronomy, Queen Mary University of London, Mile End Road, London E1 4NS, United Kingdom*

Supercritical fluids are considered to be structurally uniform with indistinguishable dynamic and thermodynamic properties across entire pressure temperature stability range. However, several recent studies suggest that the supercritical state may not be uniform and contain two distinct states of matter, liquid-like and gas-like, characterized by qualitative changes in the particle dynamics and key system properties. Here, we report direct experimental evidence of the structural crossover in a supercritical neon at pressure and temperature conditions significantly exceeding the critical point values: $250P_c$ and $6.6T_c$. The experimental results, supported by extensive molecular dynamics simulations, show disappearance of the medium-range order and qualitative change of system properties. We attribute the observed structural crossover to the Frenkel line separating liquid-like and gas-like states of supercritical matter and discuss the link between the structural crossover and qualitative changes of dynamical and thermodynamic properties. The relative width of this crossover is fairly narrow and is smaller than 10-12 % in pressure and temperature. Apart from fundamental importance of the supercritical crossover for understanding matter at extreme conditions, our results impact on advancing supercritical technologies because the Frenkel line uniquely combines maximum solubility and chemical reactivity with low viscosity and high diffusivity.

PACS numbers: 61.20.Gy, 61.20.Ne, 64.60.Kw

I. INTRODUCTION

Supercritical fluids, the state of matter above the critical point, are considered uniform in terms of structure and properties. More recently, experiments have shown that the dynamic structure factor undergoes qualitative changes in the supercritical state [1–3]. To explain this, several mechanisms were proposed which involved analogues of the liquid-gas transitions in the supercritical state: the Fisher-Widom line demarcating different regimes of decay of structural correlations [4–6]; several versions of percolation lines forming across conditional bonds or particles [7, 8]; or "thermodynamic" continuation of the boiling line such as the Widom line [9]. All these proposed mechanisms were later recognized to have issues which are not currently resolved. The Fisher-Widom line exists only in a stable fluid for model low-dimensional systems. The percolation lines are defined in realistic fluids only under specific conditions. The line of maxima of the correlation length (the Widom line) and other properties such as heat capacity, compressibility or thermal expansion depend on the path in the phase diagram and do not extend far beyond the critical point [10–13].

In 2012, a new dynamic line in the supercritical region of the phase diagram was proposed, the Frenkel line [14–17]. Crossing the Frenkel line (FL) on temperature increase (pressure decrease) corresponds to the qualitative change of particle dynamics, from the combined oscillatory and diffusive motion as in liquids to purely diffusive motion as in gases. Simultaneously, high-frequency shear rigidity disappears (transverse excitations become depleted at all frequencies), bringing the specific heat close to $c_v = 2k_B$ [17]. Other important changes take place at the liquid-like to gas-like crossover at the FL or close to it, including temperature and pressure dependencies of the speed of sound, diffusion coefficient, viscosity and thermal conductivity [16, 17].

Practically, the FL can be located on the basis of presence or absence of the velocity autocorrelation function, the criterion that coincides with $c_v = 2k_B$ [17]. The location of the FL has been calculated for several systems, including Ar, Fe, H_2O, CO_2 and CH_4 [16–20] where it was established that the temperature at the FL is about 3-5 times higher than the melting temperature at the same pressure. However, no experimental study of the Frenkel line was performed.

Importantly, the liquid-like to gas-like crossover at the FL should be accompanied by the *structural* crossover of the supercritical fluid where the details of intermediate order present in liquids close to the melting line disappear [21], yet no experimental evidence supports this prediction. Liquid structure was studied at pressures higher than the critical pressure but often at temperatures close to the melting line. Some of the previous work was aimed at elucidating the structure of supercritical water at temperature higher than the melting temperature [22]. The structure of argon was studied at high temperature and pressure [23], albeit the temperature was lower or pressure was higher than the corresponding parameters at the calculated FL. Another study of argon [24] addressed the properties in the liquid-like regime below the FL.

The sharp changes of structural parameters were not related to crossing the Frenkel line but coincided with, and were the result of, sharp changes in the chosen pressure-temperature path [25].

Experimental detection of the crossover at the FL in many interesting systems is challenging, because it requires the combination of high temperature and relatively low pressure. At these conditions, many types of standard high-pressure apparatus such as diamond anvil cells (DAC) can not be used. We have therefore chosen neon with very low melting and critical temperature ($T_c = 44.5$) and fairly high critical pressure ($P_c = 2.68$ MPa). Room temperature is 6.6 times higher than T_c, i.e. neon at room temperature and high pressure is a strongly overheated supercritical fluid. For the Lennard-Jones (LJ) fluid, the pressure corresponding to $6.6T_c$ at the FL is about $250P_c$, or $0.6 - 0.7$ GPa for neon [17]. This pressure range is suitable for the DAC.

II. METHODS

The main aim of this study is direct experimental detection of the structural crossover in supercritical neon at the FL. We employed symmetric DAC with a culet size of $300\mu m$. Re was used as gasket material and the cell was loaded with Ne at GSECARS gas-loading system [26] to an initial pressure of 0.26 GPa. The pressure was fine-controlled by membrane system and estimated by the shift of the ruby fluorescence line [27]. The x-ray diffraction experiments were performed at the GSECARS, 13-IDD beamline, APS. An incident monochromatic x-ray beam with an energy of 45 keV and $2.5 \times 3\mu m$ spot size was used. In order to suppress the Compton scattering of the diamond anvils, a multi-channel collimator (MCC) as described in [28] was employed. X-ray diffraction data was collected with a Mar345 image plate detector and the geometry was calibrated using LaB_6 standard. Collection time was about 300s. The background was measured with an empty cell prior to gas-loading.

Detector calibration, image integration and intensity corrections for oblique x-ray to detector angle, cBN seat absorption and diamond absorption were performed using Dioptas software package [29]. The resulting diffraction patterns were corrected for an additional diamond Compton scattering contribution, which was necessary because the background measurement prior to compression was measured with a thicker sample chamber than the compressed sample at high pressure. The smaller sample chamber results in more diamond in the volume of diffraction constrained by the MCC. Both the sample signal and the additional diamond compton scattering contribution were corrected with an MCC transfer function [28].

Structure factors and pair distribution functions were calculated following the procedure described in [30]. We employed the amount of diamond Compton scattering contribution in addition to the density and background scaling as an additional optimization variable. A Lorch modification function was employed during the Fourier-transform in order to minimize unphysical oscillations due to cutoff effects.

The experimental study is supported and complemented by molecular dynamics (MD) simulations. We have used the LJ potential with parameters $\sigma = 2.775$ Å and $\varepsilon = 36.831$ K [31] and simulated 4000 particles in a cubic box with periodic boundary conditions. The equilibration was first performed in the canonical ensemble at each state point, followed by the production run in the microcanonical ensemble with 0.2 fs timestep for $2 \cdot 10^6$ steps. We have simulated 15 pressure points in the range $0.05 - 3.7$ GPa, corresponding to the density range of $0.3 - 2.2$ g/cm^3. We have used LAMMPS MD simulation package [32]. The structure factors S(k) were calculated in MD simulations as Fourier transforms of the pair distribution functions $g(r)$:

$$S(k) = 1 + 4\pi \frac{N}{V} \int_0^\infty (g(r) - 1) \frac{r \sin(kr)}{k} dr, \qquad (1)$$

where N/V is the number density of fluid.

III. RESULTS AND DISCUSSION

Experimental and simulated $S(k)$ and their corresponding $g(r)$ are shown in Figure 1. We observe very good agreement between experiment and MD simulations. Figure 1(c) shows a detail view of the $g(r)$ above 6 Å. There, below 0.65 GPa the g(r) is oscillating around 1 within error bars indicating a gas like behavior, whereas above 0.65 GPa a new peak arises with pressure indicating a more long-range structure, thus, a more liquid like behavior. In order to further visualize this change, we plot the maximum of the third peak of g(r) with pressure in Figure 2 and observe two regimes: a constant value up to 0.65 GPa and a linear increase above. The regimes are additionally separated by change in slope of the position and height of the first peak of $S(k)$ (Figure S1). The crossover pressure is at 0.65 GPa as theoretically predicted [17]. Our data enables us to estimate the width of the crossover at the Frenkel line. The height and position of the first peak of $S(k)$ (see Figure S1) as well as the maximum of the third peak undergo a crossover in the range 0.65-0.99 GPa, half-width of which, 0.17 GPa, is usually taken as the maximal width of the crossover. This gives the pressure at the FL crossover can be written as $P_{\mathrm{F}} = 0.65 \pm 0.08$ GPa. Using the slope of the calculated FL (see below), this gives the crossover temperature $T_{\mathrm{F}} = 300 \pm 30$ K. Therefore, the relative width of the FL crossover in pressure and temperature is smaller

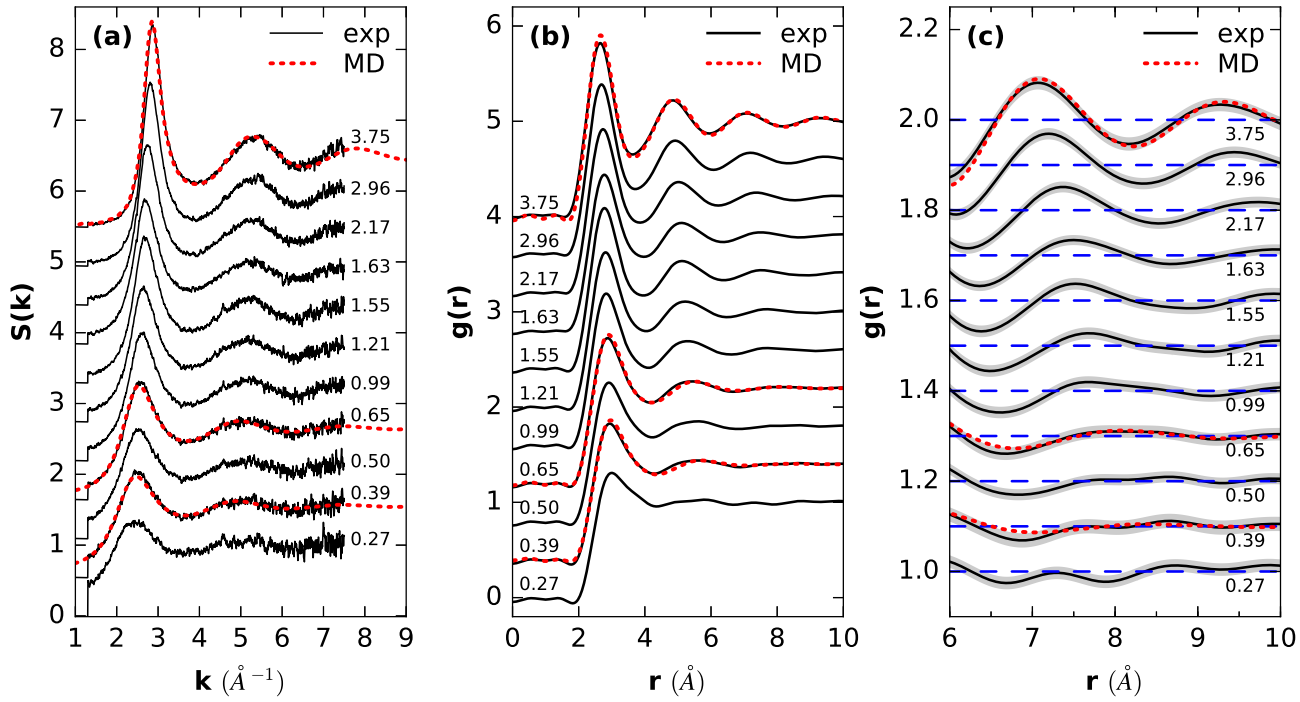

Figure 1. (a) Structure factors S(k) of neon at different pressures. (b) Radial distribution functions g(r) of neon obtained by Fourier transform of the structure factors. (c) Detail view of g(r) at large distances. The pressures are given next to the curves. The black solid and red dashed curves represent experimental (exp) and molecular dynamics (MD) data, respectively. The shaded area in (c) indicates the error, which was calculated by using the standard deviation of g(r) below the first peak; the dashed straight blue line is showing a value of 1 for each g(r) as a guide for the eye. MD radial distribution functions have been calculated with the same cutoff in S(k) as the experimental data and also using a Lorch Modification function in order to get comparable results.

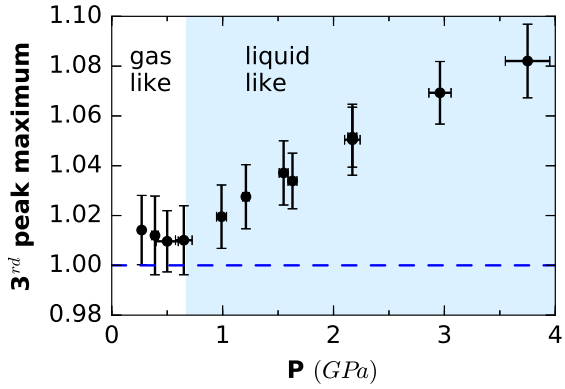

Figure 2. Maximum of the third peak of g(r) of Ne against pressure. Error bars are calculated from the standard deviation of g(r) below the first peak. Dashed blue vertical line at 1 serves as guide for the eye.

than 10-12%.

The changes of $S(k)$ and $g(r)$ reflect a modification of the medium-range order. To relate this structural crossover to the FL, we have calculated the FL using two criteria: disappearance of oscillations of velocity autocorrelation function (VAF) and $c_v = 2k_B$ [17]. VAFs are defined as $Z(t) = \frac{1}{3N}\langle\sum \frac{\mathbf{V}_i(t)\mathbf{V}_i(0)}{\mathbf{V}_i(0)^2}\rangle$ where $\mathbf{V}_i(t)$ is i-th particle velocity at time t. The heat capacities were obtained from the fluctuations of kinetic energy in microcanonical ensemble: $< K^2 > - < K >^2 = \frac{3k_B^2T^2}{2N}(1 - \frac{3k_B}{2c_V})$, where K is the kinetic energy of the system [33]. We show the examples of VAF and c_v in Fig. S2. The two criteria result in almost perfectly coinciding FL curves in Fig. 2.

From the calculations according to the two criteria above, we find that at room temperature the FL is at 0.65 ± 0.02 GPa, the same pressure where we have observed the structural crossover in our experiments and MD simulations.

The microscopic origin of the structural crossover at the FL is related to the qualitative change of particle dynamics. As discussed above, below the FL particles oscillate around quasi-equilibrium positions and occasionally jump between them. The average time between jumps is conveniently quantified by liquid relaxation time, τ. This implies that a static structure exists during τ for a large number of particles, giving rise to the well-defined

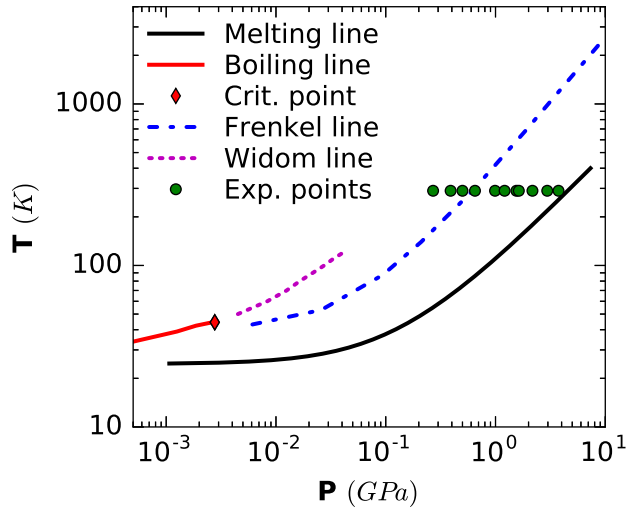

Figure 3. The calculated Frenkel line for neon, shown together with the boiling line, melting line, Widom line (calculated from maximum of heat capacity taken from [34]) and experimental points in this study.

medium-range order comparable to that existing in structurally disordered solids. This results in structural correlations at distances extending to the cage size and beyond, at distances of about 7.5 Å(see Fig. 1b). Above the FL the particles lose the oscillatory component of motion and start to move in a purely diffusive manner as in gases. This results in the loss of liquid-like medium range order, consistent with our findings.

Another interesting insight into the origin of the structural crossover comes from the relationship between structure and thermodynamics. The system energy can be written as an integral over the pair distribution function $g(r)$ as

$$E = \frac{3}{2}k_{\mathrm{B}}T + 2\pi\rho\int_0^\infty r^2U(r)g(r)dr, \qquad (2)$$

where $\rho = N/V$ is number density.

E in (2) can be written as $E = E_0 + E_T$, where E_0 is the energy at zero temperature and E_T is the thermal energy which can be represented as a sum of collective modes (phonons). The collective modes undergo the crossover at the FL, and so does the energy. In particular, the transverse modes below the FL start disappearing starting from the lowest frequency equal $\frac{1}{\tau}$ [35] and disappear completely at the FL. Above the FL, the remaining longitudinal mode starts disappearing starting from the highest frequency $\frac{2\pi c}{L}$, where L is the particle mean free path (no oscillations can take place at distance smaller than L) [35]. This gives qualitatively different behavior of the energy below and above the FL, resulting in the crossover at the FL. According to (2), the crossover of energy necessarily implies the crossover of $g(r)$.

We have confirmed this mechanism by calculating the collective modes and their dispersion curves directly. We calculate the longitudinal and transverse current correlation functions C_L and C_T as

$$C_L(k,t) = \frac{k^2}{N}\langle J_z(\mathbf{k},t)\cdot J_z(-\mathbf{k},0)\rangle$$
$$C_T(k,t) = \frac{k^2}{2N}\langle J_x(\mathbf{k},t)\cdot J_x(-\mathbf{k},0) + J_y(\mathbf{k},t)\cdot J_y(-\mathbf{k},0)\rangle$$

where $J(\mathbf{k},t) = \sum_{j=1}^{N}\mathbf{v}_j e^{-i\mathbf{k}\mathbf{r}_j(t)}$ is the velocity current [36, 37].

The maxima of Fourier transforms $\tilde{C}_L(\mathbf{k},\omega)$ and $\tilde{C}_T(\mathbf{k},\omega)$ give the frequencies of longitudinal and transverse excitations. The resulting dispersion curves are shown in Figs. 4 (a)-(c) at pressures below, nearly at and above the Frenkel line. We observe that transverse excitations are seen in a large part of the first pseudo-Brillouin zone at high pressure below the FL. At low pressure above the line, the transverse excitations disappear. At the line itself, only small traces of transverse modes close the boundary can be resolved.

We therefore find that collective excitations undergo a qualitative crossover at the FL, consistent with the earlier predictions as well as with the structural crossover via Eq. (2).

An interesting consequence of the existence of transverse modes below the FL is positive sound dispersion (PSD), the increase of the speed of sound above its adiabatic hydrodynamic value. In Figure 4 we show the adiabatic speed of sound calculated as $c_s = \gamma^{1/2}c_T$, where $c_T = \left(\frac{dP}{d\rho}\right)_T^{1/2}$ is the isothermal speed of sound and $\gamma = c_P/c_V$ is the ratio of isobaric and isochoric heat capacities. The isobaric heat capacity was calculated as $c_P = c_V + \frac{T}{\rho^2}\left(\frac{\partial P}{\partial T}\right)_\rho^2\left(\frac{\partial P}{\partial \rho}\right)_T^{-1}$. We observe the PSD below the FL but not above. This effect can be explained due to the main contribution to PSD coming from the shear modulus at high frequencies [35]. If the dependence of the bulk modulus on frequency is weak, i.e. $B(\omega) \approx B(0)$ then magnitude of the PSD can be evaluated by using the following relationship [35]:

$$v_l^2 = c_s^2 + \frac{4}{3}v_t^2 \qquad (3)$$

where v_l is the speed of longitudinal waves, v_t is the speed of transverse excitations and c_s is the hydrodynamics speed of sound in the limit of low k (long waves).

From the calculated dispersion curves in Fig. 4 we find $v_l = 3240 \pm 50$ m/s, $v_t = 1160 \pm 100$ m/s. Using Eq. 3 at $k = 0.8$ Å^{-1} where the magnitude of PSD is maximal and

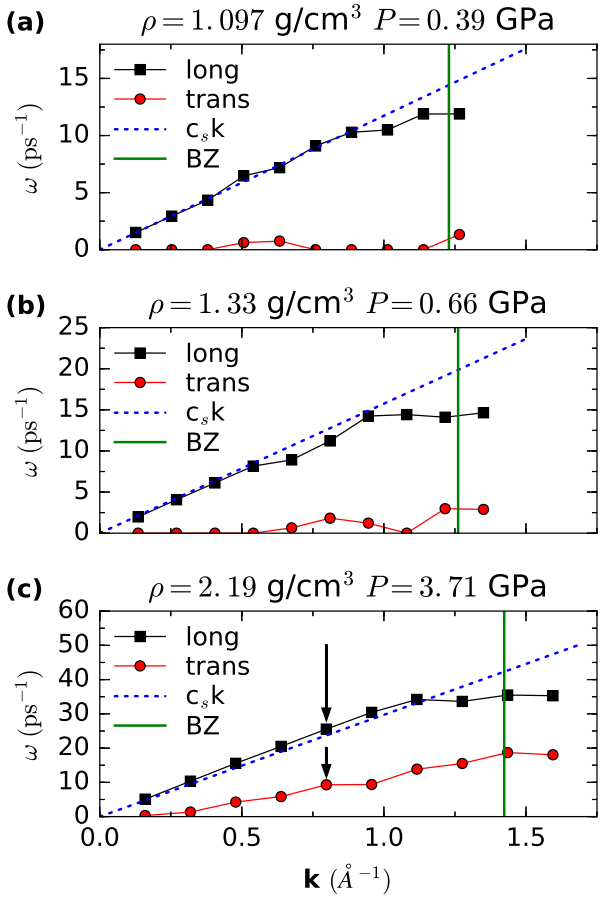

Figure 4. Excitation spectra of neon at pressure points (a) above (b) nearly at and (c) below the Frenkel line. Longitudinal (squares) and transverse (circles) spectra are shown. The dashed lines give the Debye dispersion law $\omega = c_s k$, where c_s is adiabatic speed of sound. The vertical lines mark the boundary of pseudo-Brillouin zone. The arrows at panel (c) indicate the k point where PSD was calculated.

c_s calculated to be 2970 ± 10 m/s, we find $v_l = 3260 \pm 100$ m/s.

Therefore, PSD below the FL can be quantitatively described by the visco-elastic model as a result of the presence of transverse modes in the supercritical system, although we recall other explanations of this effect. Observing the change of the dynamic structure factor [1–3] and PSD, it was proposed to relate the change to the Widom line [9]. However, we note that the Widom line exists close the critical point only and disappears deeply inside the supercritical region as is the case here [10–13].

An interesting consequence of our results is the possibility to observe liquid-liquid phase transitions in the supercritical state. So far liquid-liquid transitions involving the change of the medium-range order have been observed below the critical point only [38]. In this work, we have ascertained that the medium-range is present in the supercritical state too, as long as the system is below the FL. Therefore, we propose that liquid-liquid phase transitions can be observed above the critical point below the FL.

We propose that our results can be relevant for industrial application of supercritical technologies [39]. Supercritical fluids combine high density ($2-3$ times higher than the density at the triple point) and high diffusion coefficient that are orders of magnitude higher than those of subcritical liquids. This leads to remarkable increase of solubility and speedup of chemical reactions. Interestingly, the solubility maxima lie very close to the Frenkel line [20]: increasing pressure along the FL gives higher density and diffusivity and minimal viscosity. The data of the FL can enhance the supercritical technologies, particulary at higher pressure in the range $1-3$ GPa where high-pressure chambers can have large volume.

In summary, we have directly ascertained the structural crossover in the supercritical state. Of particular importance is that the crossover operates at extremely high pressure and temperature: $6.6T_c$ and $250P_c$. The relative width of the crossover is fairly narrow and is less than 10 % in both pressure and temperature. This enables us to consider the FL as the boundary between the liquid-like and gas-like states of supercritical matter.

ACKNOWLEDGEMENTS

We are grateful to G. Simeoni, V. N. Ryzhov, E. N. Tsiok and J. E. Proctor for fruitful discussions. Yu.D.F. thanks the Russian Scientific Center at Kurchatov Institute and Joint Supercomputing Center of Russian Academy of Science for computational facilities. Yu.D.F. (molecular dynamic simulations, the discussions of the results, writing paper) and V.V.B. (formulation of the problem, the discussions of the results, writing paper) are grateful to Russian Science Foundation (14-22-00093) for the financial support. We thank S. Tkachev for his help during gas-loading. Use of the COMPRES-GSECARS gas loading system was supported by COMPRES under NSF Cooperative Agreement EAR 11-57758 and by GSECARS through NSF grant EAR-1128799 and DOE grant DE-FG02-94ER14466. Portions of this work were performed at GeoSoilEnviroCARS The University of Chicago, Sector 13), Advanced Photon Source (APS), Argonne National Laboratory. GeoSoilEnviroCARS is supported by the National Science Foundation - Earth Sciences (EAR-1128799) and Department of Energy- GeoSciences (DE-FG02-94ER14466). This research used resources of the Advanced Photon Source, a U.S. Department of Energy (DOE) Office of Science User Facility operated for the DOE Office of Science by Argonne National Laboratory under Contract No. DE-AC02-06CH11357.

[1] F. Bencivenga, a. Cunsolo, M. Krisch, G. Monaco, G. Ruocco, and F. Sette, EPL **75**, 70 (2006).

[2] F. Gorelli, M. Santoro, T. Scopigno, M. Krisch, and G. Ruocco, Phys. Rev. Lett. **97**, 15 (2006), arXiv:0611044 [cond-mat].

[3] G. G. Simeoni, T. Bryk, F. a. Gorelli, M. Krisch, G. Ruocco, M. Santoro, and T. Scopigno, Nature Phys. **6**, 503 (2010).

[4] M. E. Fisher and B. Widom, J. Chem. Phys. **50**, 3756 (1969).

[5] C. Vega, L. F. Rull, and S. Lago, Phys. Rev. E **51**, 3146 (1995).

[6] M. Smiechowski, C. Schran, H. Forbert, and D. Marx, Phys. Rev. Lett. **116**, 1 (2016).

[7] M. Bernabei, A. Botti, F. Bruni, M. A. Ricci, and A. K. Soper, Phys. Rev. E **78**, 1 (2008).

[8] M. Bernabei and M. A. Ricci, J. Phys. Cond. Matt. **20**, 494208 (2008).

[9] L. Xu, P. Kumar, S. V. Buldyrev, S.-H. Chen, P. H. Poole, F. Sciortino, and H. E. Stanley, Proc. Natl. Acad. Sci. U.S.A. **102**, 16558 (2005), arXiv:0509616 [cond-mat].

[10] V. V. Brazhkin, Y. D. Fomin, A. G. Lyapin, V. N. Ryzhov, and E. N. Tsiok, J. Phys. Chem. B **115**, 14112 (2011).

[11] V. V. Brazhkin and V. N. Ryzhov, J. Chem. Phys. **135** (2011), 10.1063/1.3627231, arXiv:1104.2973.

[12] Y. D. Fomin, V. N. Ryzhov, E. N. Tsiok, and V. V. Brazhkin, Phys. Rev. E **91**, 1 (2015).

[13] V. V. Brazhkin, Y. D. Fomin, V. N. Ryzhov, E. E. Tareyeva, and E. N. Tsiok, Phys. Rev. E **89**, 1 (2014), arXiv:1402.6540 [cond-mat.soft].

[14] V. V. Brazhkin, A. G. Lyapin, V. N. Ryzhov, K. Trachenko, Y. D. Fomin, and E. N. Tsiok, Physics-Uspekhi **55**, 1061 (2012).

[15] V. V. Brazhkin, Y. D. Fomin, a. G. Lyapin, V. N. Ryzhov, and K. Trachenko, JETP Lett. **95**, 164 (2012).

[16] V. V. Brazhkin, Y. D. Fomin, A. G. Lyapin, V. N. Ryzhov, and K. Trachenko, Phys. Rev. E **85**, 1 (2012), arXiv:1104.3414.

[17] V. V. Brazhkin, Y. D. Fomin, A. G. Lyapin, V. N. Ryzhov, E. N. Tsiok, and K. Trachenko, Phys. Rev. Lett. **111**, 1 (2013).

[18] D. Fomin, V. N. Ryzhov, E. N. Tsiok, and V. V. Brazhkin, Sci. Rep. **5**, 14234 (2015), arXiv:arXiv:1502.02939v1.

[19] Y. D. Fomin, V. N. Ryzhov, E. N. Tsiok, V. V. Brazhkin, and K. Trachenko, Sci. Rep. **4**, 7194 (2014).

[20] C. Yang, V. V. Brazhkin, M. T. Dove, and K. Trachenko, Phys. Rev. E **91**, 1 (2015), arXiv:1502.07910.

[21] D. Bolmatov, V. V. Brazhkin, Y. D. Fomin, V. N. Ryzhov, and K. Trachenko, J. Chem. Phys. **139** (2013), 10.1063/1.4844135, arXiv:arXiv:1308.1786v1.

[22] A. K. Soper, Chem. Phys. **258**, 121 (2000).

[23] M. Santoro and F. Gorelli, Phys. Rev. B **77**, 212103 (2008).

[24] D. Bolmatov, M. Zhernenkov, D. Zav, S. N. Tkachev, A. Cunsolo, and Y. Q. Cai, Sci. Rep. **5**, 1850 (2015), arXiv:1502.03877v1.

[25] V. V. Brazhkin and J. E. Proctor, ArXiv e-prints (2016), arXiv:1608.06883 [cond-mat.soft].

[26] M. Rivers, V. Prakapenka, A. Kubo, C. Pullins, C. Holl, and S. Jacobsen, High Press. Res. **28**, 273 (2008).

[27] H. K. Mao, J. Xu, and P. M. Bell, J. Geophys. Res. **91**, 4673 (1986).

[28] G. Weck, G. Garbarino, S. Ninet, D. Spaulding, F. Datchi, P. Loubeyre, and M. Mezouar, Rev. Sci. Instr. **84**, 063901 (2013).

[29] C. Prescher and V. B. Prakapenka, High Press. Res. **35**, 223 (2015).

[30] J. Eggert, G. Weck, P. Loubeyre, and M. Mezouar, Phys. Rev. B **65**, 174105 (2002).

[31] S. K. Oh, J Thermodyn. **1** (2013), 10.1155/2013/828620.

[32] S. Plimpton, J. Comp. Phys. **117**, 1 (1995).

[33] D. Frenkel and B. Smit, *Understanding Molecular Simulation* (Academic Press, 2002) p. 638.

[34] E. Lemmon, M. McLinden, and D. G. Friend, in *NIST Chemistry WebBook, NIST Standard Reference Database Number 69*, edited by P. Linstrom and W. Mallard (National Institute of Standards and Technology, Gaithersburg MD, 20899).

[35] K. Trachenko and V. V. Brazhkin, Rep. Prog. Phys. **79**, 16502 (2016), arXiv:1512.06592.

[36] J. P. Hansen and I. R. McDonald, *Theory of Simple Liquids*, 4th ed. (Academic Press, 2013) p. 636.

[37] D. C. Rapaport, *The Art of Molecular Dynamics Simulations* (Cambridge University Press, 1995) p. 564.

[38] V. V. Brazhkin, S. V. Buldyrev, V. N. Ryzhov, and H. E. Stanley, eds., *New Kinds of Phase Transitions: Transformations in Disordered Substances, Proceeding of NATO Advanced Research Workshop, Volga River* (Kluwer Academic Publishers, 2002).

[39] E. Kiran, P. Debenedetti, and C. J. Peters, *Supercritical Fluids* (Springer-Science+Business Media, BV, 2000) p. 596.

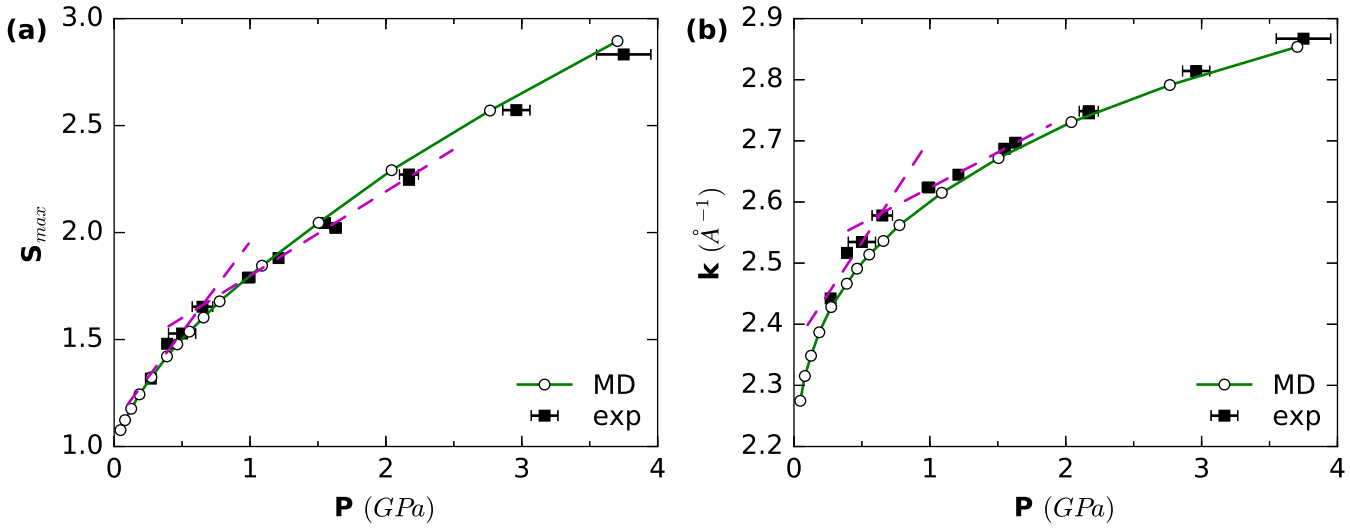

Figure S1. Extracted height (a) and position (b) of the first maximum of the structure factor S(k) against pressure. MD results are shown as connected circles and experimental results are shown as black squares. The dashed magenta lines show the difference in slopes below and above the crossover of the experimental data.

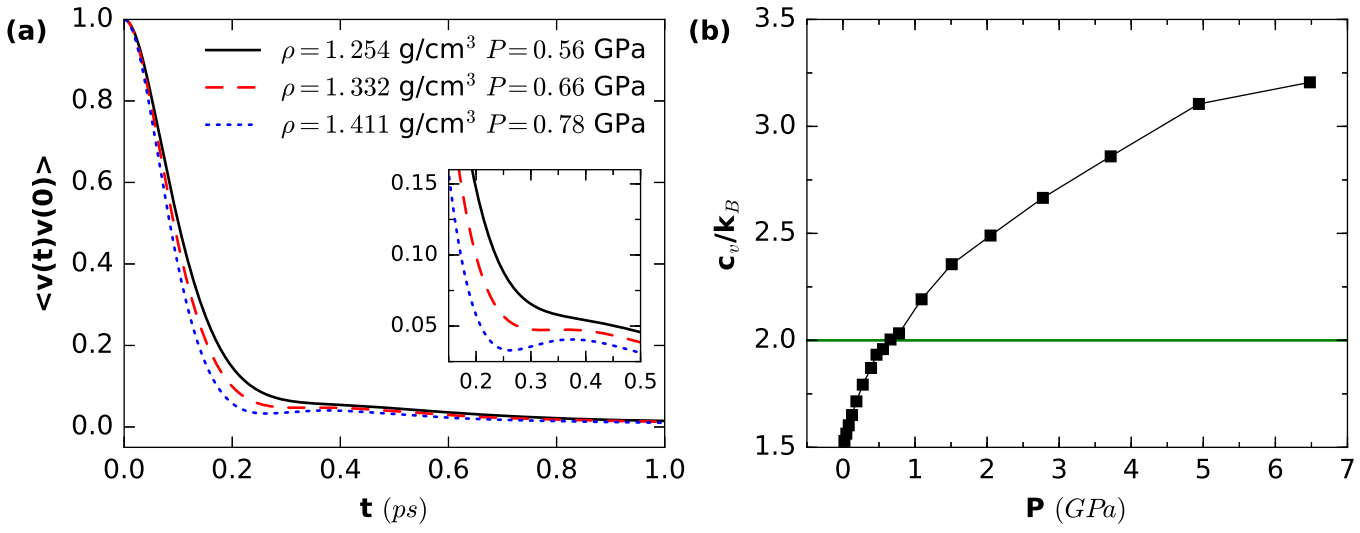

Figure S2. (a) Velocity autocorrelation functions of Ne in the vicinity of the crossover pressure. (b) Isochoric heat capacities of neon at $T = 290$ K. The horizontal line marks $c_v = 2k_{\mathrm{B}}$.